Toward Acoustic-Based Normalization of Laryngeal EMG for Improved Interspeaker Consistency in Muscle-to-Acoustic Mapping

*Josué D. Martínez, †Emiro J. Ibarra, †Jesús A. Parra, ‡,§Daryush D. Mehta, ‡,§James T. Heaton, ‡,§Robert E. Hillman, ‡,§Michal J. Plocienniczak, ‡Jameson C. Cooper, and *Matías Zañartu, *†*Valparaiso, Chile, and* ‡§*Boston, USA*

SUMMARY: Understanding how intrinsic laryngeal muscle activation relates to vocal output is essential for advancing experimental voice research. However, intrasubject variability remains a major challenge when comparing EMG recordings across sessions. To address this, a normalization framework based on acoustic targets was implemented to improve the consistency of EMG-acoustic relationships across sessions. Signals from the cricothyroid (CT), thyroarytenoid (TA), and lateral cricoarytenoid (LCA) muscles were collected across four sessions from a healthy adult performing a set of phonatory and non-phonatory vocal tasks. Muscle Activation Plots (MAPs) were generated to visualize the relationship between normalized EMG activity and acoustic outcomes, specifically fundamental frequency (f_o) and sound pressure level (SPL). Compared to traditional peak-based normalization, the proposed method reduced intrasubject variability and improved intersession consistency in the EMG-f_o relationship, as reflected by an increase in ICC from 0.52 to 0.83 and a reduction in MAE from 84.87 Hz to 19.23 Hz. These findings represent a step toward more consistent intramuscular EMG normalization and improved interpretation of muscle-specific control strategies in human voice production.

Keywords: Intramuscular electromyography–Normalization–Intrasubject variability–Fundamental frequency–Acoustic targets–Muscle activation plots–Intrinsic laryngeal muscles.

INTRODUCTION

Studying laryngeal neuromuscular control is essential for understanding the biomechanics of voice production, respiration, and airway protection. The larynx is composed of cartilaginous structures and intrinsic laryngeal muscles (ILM) that regulate the tension and position of the vocal folds (VF), facilitating phonation and other fundamental laryngeal functions. The ILM, including the thyroarytenoid (TA) and cricothyroid (CT), play a primary role in modulating fundamental frequency (f_o),[1] while the lateral cricoarytenoid (LCA) and interarytenoid (IA) muscles primarily contribute to regulating sound pressure level (SPL) and glottal closure.[2] The posterior cricoarytenoid (PCA), in contrast, is the sole abductor of the VF and facilitates glottal opening.[3]

Laryngeal muscle activity has been extensively investigated in animal studies, particularly in canines, to elucidate the roles of ILM in controlling VF tone and tension under controlled neurophysiological and biomechanical conditions.[4–7] These studies have shown that CT activation contributes to VF elongation and increased f_o,[8] while TA activation may either raise or lower f_o, depending on the level of CT co-activation.[4,9] Specifically, TA stiffens the VF and raises f_o at low CT levels, but may reduce f_o at high CT activation by lowering tension in the cover layer. The LCA and IA muscles primarily facilitate posterior glottal closure, contributing to phonation onset.[5,9] When co-activated with the CT, the LCA/IA complex further stabilizes the glottis under high-strain conditions, enabling greater f_o values.[10]

However, limitations have been identified in these studies, as canine structures are relied upon, which, despite anatomical similarities, exhibit geometric and mass distribution differences in ILM compared to humans, and these differences are considered to potentially influence VF vibration and the range of achievable f_o values.

Computational models have been developed to study how ILM activations influence phonatory outcomes such as f_o and SPL. The three-mass VF model, for instance, linked muscle activation to VF adjustments and successfully reproduced oscillatory behavior consistent with physiological data.[11–13] More advanced frameworks, including body-cover and finite element models,[14–17] have enabled simulation of layered VF structures and muscle coordination under controlled conditions. While these models offer valuable insights into neuromuscular control, their interpretability is constrained by simplifications in muscle properties and limited representation of intra and intersubject variability.[18–20]

On the other hand, research on human subjects using intramuscular EMG has been constrained by the technical

Accepted for publication August 8, 2025.

From the *Department of Electronic Engineering, Universidad Técnica Federico Santa María, Valparaíso 23400003, Chile; †Department of Electronic Engineering and Advanced Center for Electrical and Electronic Engineering, Universidad Técnica Federico Santa Maria, Valparaiso 2390123, Chile; ‡Center for Laryngeal Surgery and Voice Rehabilitation, Massachusetts General Hospital, Boston, MA, USA; and the §Department of Surgery, Harvard Medical School, Boston, MA, USA.

Address correspondence and reprint requests to: Josué D. Martínez, Department of Electronic Engineering and Advanced Center for Electrical and Electronic Engineering, Universidad Técnica Federico Santa Maria, Valparaiso 2390123, Chile. E-mail: josue.martinez@usm.cl

Journal of Voice, Vol xx, No xx, pp. xxx–xxx
0892-1997

https://doi.org/10.1016/j.jvoice.2025.08.014

complexity and invasive nature of the procedure. Fine-wire and multichannel recording methods have been employed to analyze electrical activity in ILMs during phonatory and non-phonatory tasks, examining muscle activity in patients with laryngeal dystonia as well as in healthy individuals.[1,21–23] Correlations between muscle activation patterns and VF movement have been observed during speech and nonspeech gestures, illustrating the complex relationship between neuromuscular control and phonatory outcomes.[24,25] Specifically, pitch glides have been shown to strongly recruit the CT muscle, whose activation increases progressively with f_o.[26] In contrast, tasks involving increased loudness or elevated P_s, such as high-intensity vowel phonation, descending /pae/ gestures, or voluntary glottal closure, have been associated with increased activation of the TA and LCA muscles.[27,28] These findings support the differential contributions of individual ILMs depending on the acoustic dimension being modulated, providing a functional rationale for selecting muscle-specific tasks during normalization procedures.

To compare EMG amplitude across individuals, muscles, or recording sessions, signal normalization is required due to anatomical and physiological factors known to significantly affect EMG amplitude.[29] Traditionally, intramuscular EMG normalization for ILM has relied on the maximum EMG amplitude obtained during a Maximum Voluntary Isometric Contraction (MVIC).[24,30] Other studies have employed average activation values under defined subglottal pressure conditions to normalize EMG activity[28]. However, this approach presents limitations, primarily due to the lack of a standardized task capable of consistently eliciting maximal muscle activation across sessions. Additionally, variability in f_o and subglottal pressure(P_s) across sessions or in pathological subjects can lead to different EMG maximum amplitudes for the same phonatory task, complicating within-subject comparisons over time.[1,22]

In studies involving muscles from other anatomical regions, alternative techniques, such as force targets or task-specific normalization procedures, have been used to standardize effort, often relying on the mean or peak EMG amplitude during those tasks (Mean_{Task} or Peak_{Task}) as normalization references across sessions.[31,32] However, such mechanical proxies are not readily available or meaningful for ILMs, whose function is tightly linked to aerodynamic and acoustic control of voice production. Unlike limb muscles, ILMs do not generate easily isolated force outputs. Instead, their coordination produces complex vocal outcomes, most notably, variations in f_o and SPL, that are readily measurable and reflect the functional role of specific muscles during speech and voice tasks. Therefore, we proposed an alternative normalization approach based on acoustic variables, f_o and SPL, that align with the mechanisms of voiced sound production. This task-based strategy provides interpretable outcomes of ILM activity during phonatory tasks involving vocal fold vibration.

The present study explores the relationship between the activation of ILM, specifically the CT, TA, and LCA, and two acoustic features of phonation (f_0 and SPL). Using intramuscular EMG recordings and acoustic measurements, this study pursues two main objectives. The first is to address the challenge of intrasubject variability in ILM activation by developing an acoustic-based normalization approach for in vivo human EMG recordings, thereby enabling consistent comparisons within and across recording sessions for the same participant. The second objective is to map these normalized EMG patterns to f_o and SPL, helping to understand their functional relationships. This approach establishes a foundation for future research in vocal physiology and biomechanical modeling, and is well-suited for extension to inter-subject analyses in subsequent studies.

MATERIALS AND METHODS

Participant demographics and experimental protocol

A 71-year-old healthy male volunteer with no history of dysphonia or laryngeal abnormalities participated in the study. This individual is a professor and a habitual voice user. Informed consent was obtained from the participant, and the experimental protocols were approved by the institutional review board of the Massachusetts General Hospital, Boston.

Before EMG electrode insertion, the participant underwent training to practice the required phonatory tasks. The experimental procedure consisted of four separate sessions, during which the participant performed a total of three phonatory task sets, along with non-phonatory and combined tasks, as detailed in Table 1.

TABLE 1.
Experimental protocol. The phonatory tasks are categorized into three sets: sustained vowels, pitch glides, and repeated syllable tasks, with variations in pitch and loudness conditions indicated. Non-phonatory and combined tasks are also listed.

Category	Task	Pitch	Loudness
Phonatory Set 1	Sustained vowels /a/, /i/	Low, Habitual, High	Comfortable
		Habitual	Soft, Loud
Phonatory Set 2	Pitch glides on /a/, /i/	Ascending, Descending	Comfortable
Phonatory Set 3	Repeated /pae/, /pi/	Low, Habitual, High	Loud to Soft
Non-Phonatory	Cough, Swallow, Throat clear		
Combined	Vowel + Valsalva maneuver	Habitual	Very Loud

The selection of tasks was guided by their relevance in prior literature and their ability to elicit distinct patterns of ILM activation. Phonatory Set 1 involved sustained vowel productions (/a/ and /i/) lasting 5 s under varying pitch (low, habitual, high) and loudness (soft, comfortable, loud) conditions. These tasks are commonly used to assess steady-state ILM activation across acoustic conditions.[33] Phonatory Set 2 consisted of ascending and descending pitch glides on the same vowels at comfortable loudness, designed to preferentially activate the CT muscle.[26,25,30,21] In Phonatory Set 3, repeated syllables (/pae/, /pi/) were produced at three pitch levels (low, habitual, high), with either sustained loudness or a progressive reduction from loud to soft. These syllables were selected to elicit dynamic TA and LCA activation under vocal effort variations inherently driven by changes in P_s.[28]

Non-phonatory gestures included coughing, swallowing, throat clearing, and chin tuck. The combined task consisted of vowel production during a Valsalva maneuver, performed at habitual pitch and very loud intensity. These high-effort tasks were selected to elicit maximal activation of ILM, particularly the TA and LCA, providing reference points for traditional maximum-based normalization across sessions.[34]

Data acquisition protocol

To measure muscle activity, bipolar hooked-wire electrode pairs were inserted into three ILM: two VF adductors (TA and LCA) and the VF tensor (CT).[35]Table 2 shows the muscles recorded in each session, grouped by VF laterality (left and right). In several sessions, two bipolar electrode pairs were inserted into the same muscle to assess potential spatial variation in intramuscular activation. These placements are labeled with numeric identifiers (e.g., TA1 and TA2) to distinguish separate electrode insertions in the same muscle during a single session.

In all sessions, pre-sterilized disposable hooked-wire electrode pairs were inserted into ILM using a 27-gauge, 30 mm-long hypodermic carrier needle (221–28SS-730, Rhythmlink International LLC). These stainless-steel, enamel-insulated wires were 44 gauge (.002″ diameter) with approximately 2 mm of exposed metal at the bent-over (i.e., hooked) ends that extended 2–6 mm from the carrier needle.

TABLE 2.
Recorded ILM by session, grouped by VF laterality (left and right). For sessions where the same muscle was recorded with two bipolar electrode pairs, the placements are differentiated by numbers (e.g., TA1 and TA2).

Session	Left Side Muscles	Right Side Muscles
1	CT	CT, TA, LCA
2	CT, TA1, TA2, LCA	CT, TA1, TA2
3	CT, TA1, TA2, LCA1, LCA2	CT, TA, LCA
4	CT1, CT2, TA, LCA	CT1, CT2, TA

Note: CT = cricothyroid; TA = thyroarytenoid; LCA = lateral cricoarytenoid.

The carrier needles were inserted through the neck skin at the cricothyroid gap location. When targeting the CT, the needle was inserted approximately 5 mm lateral to the neck midline at the cricothyroid gap, angled about 50° from the sagittal plane, with a penetration depth of about 15 mm. When targeting the TA or LCA, the needle was inserted at the neck midline at the cricothyroid gap, angled about 30° from the sagittal plane, and passed lateral to the cricothyroid membrane without entering the airway (e.g., remaining submucosal). After passing through the cricothyroid space, the needle was directed either superiorly and laterally toward the TA muscle, or directed more posteriorly, less superiorly, and laterally towards the LCA muscle, to depths of approximately 20 and 26 mm, respectively.[24,36]

Hooked-wire electrode placement was estimated using verification gestures for each targeted muscle. Both the TA and LCA demonstrated burst activity at phonation onset,[22] with the TA having a more sustained increase in activity throughout glottic closure than the LCA muscle. The CT muscle placement was verified by significantly increased activation during high-pitch phonation, little activity during low-pitch phonation, and the absence of activity during swallowing, confirming no contamination of the CT signals with strap muscle activity. Although electrode placement was guided by anatomical landmarks and standardized insertion techniques, precise localization of each electrode pair could not always be confirmed unequivocally. Signal-based criteria for validating electrode co-localization are described in the following subsections.

Muscle activity was recorded using an 8-channel EMG system (Bagnoli, Delsys Inc., Natick, MA) with small expansion springs for attaching the fine wires. Electrical ground was provided by a 2.5″ diameter pad electrode applied to the dorsal neck at approximately the C6 and C7 vertebrae. The system band-pass filtered the differential EMG signal from each hooked-wire pair at 20–450 Hz and applied a 1000x gain before digitization at 20 kHz (Digidata® 1440, Molecular Devices, San Jose, CA).

An omnidirectional acoustic microphone (model MKE104, manufactured by Sennheiser Electronic GmbH®, Wennebostel, Germany) was positioned 15 cm from the lips. Acoustic and EMG signals were synchronously recorded and calibrated to physical units: sound pressure in pascals (Pa) for the microphone and voltage (V) for the EMG signals.

Signal processing for acoustic and EMG features

Acoustic-based features

Both SPL and f_o were computed from 50 ms analysis windows of the calibrated acoustic signal, with a 25 ms overlap between consecutive frames. SPL was derived from the root mean square value of each windowed segment of the microphone signal, recorded at a distance of 15 cm from the lips.[37] The f_o was extracted using MATLAB's

pitch function, applying the Log-Harmonic Summation (LHS) method.[38]

EMG signal processing and electrode identification

The raw EMG signals were first high-pass filtered using a fourth-order Butterworth filter (10 Hz).[29] The filtered signals were then full-wave rectified and subsequently low-pass filtered at 8 Hz to obtain the amplitude envelope, as described in.[24] The resulting envelope was segmented into 50 ms windows with 25 ms overlap, and the mean EMG amplitude was extracted from each segment. These segments were then synchronized with the corresponding acoustic windows, producing time-aligned EMG-acoustic segments.

To identify electrode pairs likely inserted into the same muscle, cross-correlation was applied to the raw EMG signals under the assumption that high temporal similarity indicates spatial proximity and potential crosstalk between nearby channels.[39,40] A cross-correlation threshold of 0.5 was used to infer co-localization within the same muscle. Additionally, Pearson correlation coefficients (r) were calculated between all pairs of EMG envelopes. A strong negative correlation with CT activation ($r < -0.5$) was used to help differentiate TA muscle, based on their known antagonistic roles during pitch modulation.[30,41] For LCA identification, envelope-based correlation was insufficient. Consequently, qualitative inspection of EMG envelopes was performed during tasks with stable adductory demand—specifically, /pae/ descending and /ifi/. Channels exhibiting sustained envelope amplitude with limited modulation across these tasks were considered representative of LCA activity.

Normalization procedure

The normalization procedure used in this study was grounded in the principles of submaximal task-based normalization,[42,43,31] based on acoustic targets (f_o and SPL). This approach has been proposed as an alternative to MVIC techniques for dynamic and task-specific EMG applications, particularly to reduce intrasubject variability. Given that each acoustic target may be associated with different levels of EMG activation, due to varying combinations of subglottal pressure and co-activation of other ILM, normalization was performed by grouping EMG-acoustic segments into non-overlapping 1 Hz bins for f_o (CT) and 1 dB bins for SPL (TA and LCA). Within each bin, the maximum EMG amplitude was extracted to represent a pattern of peak EMG amplitudes across the acoustic range. The corresponding EMG normalization value was obtained by linearly interpolating between these peak values and the acoustic target. To this end, phonatory tasks that elicited the highest activation levels were used for each muscle.

For the CT muscle, maximum activation was associated with pitch glide tasks from Phonatory Set 2,[26,30,21,41] which typically produce the highest f_o values. In contrast, for the TA and LCA muscles, both involved in glottal adduction and P_s regulation, maximum activation was associated with high SPL values,[33,27] which are generally achieved during high-intensity productions such as increasing the loudness of /pae/ gestures performed in Phonatory Set 3.[28] Only phonatory gestures involving vocal fold vibration were considered, as these tasks are directly related to voiced sound production and better reflect the functional role of ILM during speech.

For comparison purposes, a traditional normalization approach was also implemented. In this method, each muscle's EMG signal was normalized by dividing it by the maximum amplitude observed within the session, regardless of the task. The peak value was selected from the highest activation measured across all available tasks, including both phonatory and non-phonatory conditions, such as swallowing and Valsalva maneuvers, performed during that session.[24,30,25] To ensure the reliability of the extracted measures, the raw EMG signals were manually reviewed to confirm that the selected maximum values were not affected by non-EMG events, such as motion artifacts. When such artifacts were identified within a trial, that specific trial was excluded from the normalization process, while retaining the remaining repetitions of the corresponding task. Both approaches were applied in parallel to compare proposed normalization outcomes in downstream analyses, as shown in the Results section.

Muscle-acoustic mapping consistency across sessions

To assess the repeatability of muscle-acoustic relationships across sessions, muscle activation plots (MAPs) were generated using normalized EMG activation values and interpolated acoustic features.[15,11] Each MAP represents a two-dimensional grid of activation for two muscles being compared, with color-coded values indicating either f_o or SPL. Three configurations were analyzed: (1) CT vs. TA with f_o, (2) CT vs. TA with SPL, and (3) LCA vs. CT with f_o. MAPs were computed independently for each session and for both normalization strategies (traditional and proposed). To enable cross-session comparison, a shared activation region was identified within each configuration. Each session was treated as a repeated measure, yielding four values per grid point in the overlapping region. MAPs offer a structured and interpretable framework for evaluating whether normalization strategies preserve consistent and meaningful activation-acoustic relationships across sessions.

To evaluate intrasubject variability, pairwise comparisons were performed across all combinations of the four recording sessions (i.e., S1-S2, S1-S3, …, S3-S4), resulting in six session pairs. For each pair, acoustic values (f_o or SPL) were extracted from the common MAP region and compared using Pearson correlation (r), mean absolute error (MAE), and root mean square error (RMSE). In addition, global consistency across all sessions was assessed

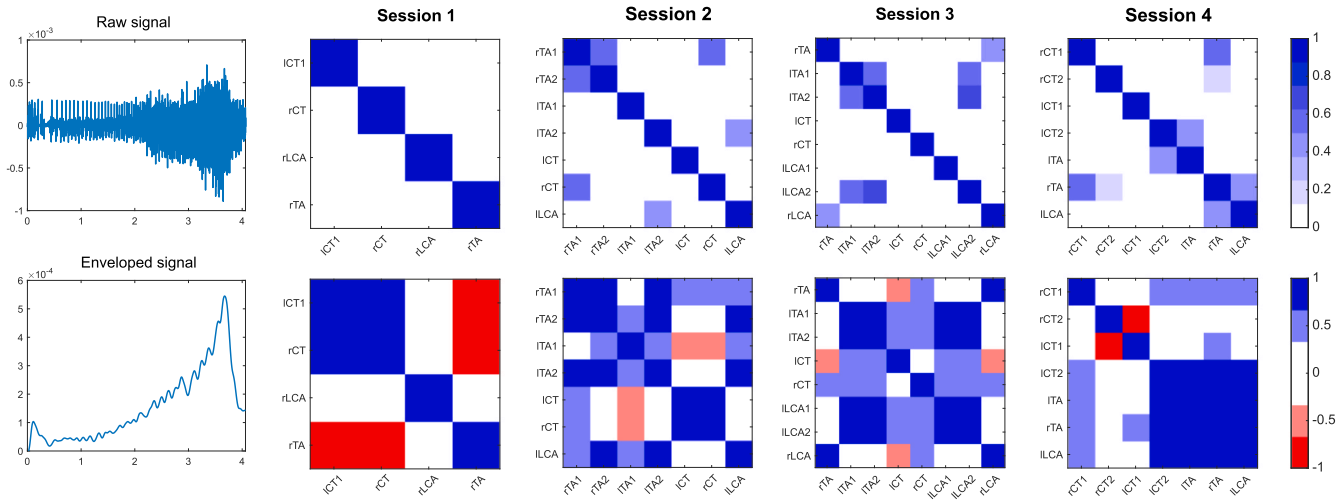

FIGURE 1. (Top row) Cross-correlation matrices computed from raw EMG signals. (Bottom row) Pearson correlation matrices computed from enveloped EMG signals across four recording sessions. Each matrix represents the correlation between electrode pairs placed within ILMs.

using intraclass correlation coefficient (ICC, model 2,1) and coefficient of variation (CoV).

RESULTS

Correlation-based channel selection

Channel selection was guided by both cross-correlation of raw EMG signals and Pearson correlation coefficients of EMG envelopes, in accordance with the thresholds defined in the EMG signal processing methodology (Section 2.3.2). The resulting correlation heatmaps are presented in Figure 1. In the top row, cross-correlation matrices computed from raw EMG signals revealed spatial patterns that were consistent across all tasks within each session. Most channel pairs exhibited low correlation ($r > 0.1$), indicating substantial functional independence. However, electrode pairs with correlation values exceeding 0.5 were interpreted as co-localized within the same muscle, reflecting spatial proximity and potential crosstalk. [40,39]

The bottom row displays *r*-value matrices derived from EMG envelopes recorded during pitch glide descending tasks across all sessions, capturing co-activation patterns. A consistent strong negative correlation ($r < -0$-.5) was observed between CT and TA in some electrode pairs during descending glides, reflecting their well-established biomechanical antagonism in pitch modulation. This behavior was used to distinguish TA from LCA electrodes.

Based on spatial and functional correlation patterns, one representative CT, TA, and LCA channel triplet was selected per session: rCT-rTA-rLCA (Session 1), lCT-lTA1-lLCA (Session 2), lCT-rTA-lLCA2 (Session 3), and lCT1-rCT2-lTA (Session 4).

Acoustic-based EMG normalization

Figure 2 displays the mean of maximum EMG amplitudes for the CT, TA, and LCA muscles across four recording sessions and multiple tasks, including both phonatory and non-phonatory gestures. For traditional normalization, the task yielding the highest EMG value was used as the reference for each muscle. In the case of CT, this corresponded to the pitch glide task (Phonatory Set 2), which

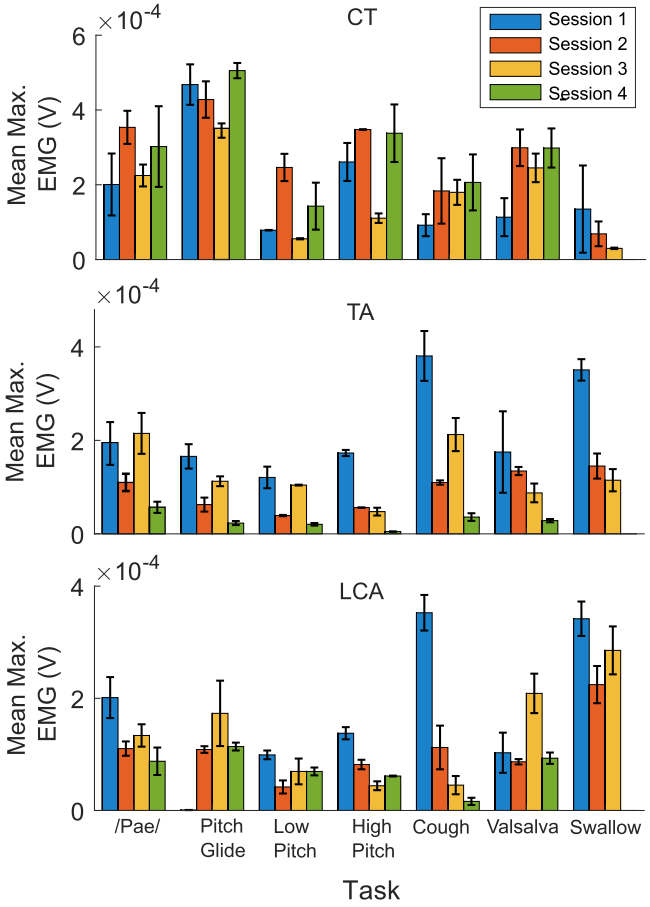

FIGURE 2. Comparative bar plot of mean maximal CT, TA and LCA muscle activation values from EMG signal envelope data. The results of each session per phonatory and non-phonatory task (Valsalva and swallow) are shown.

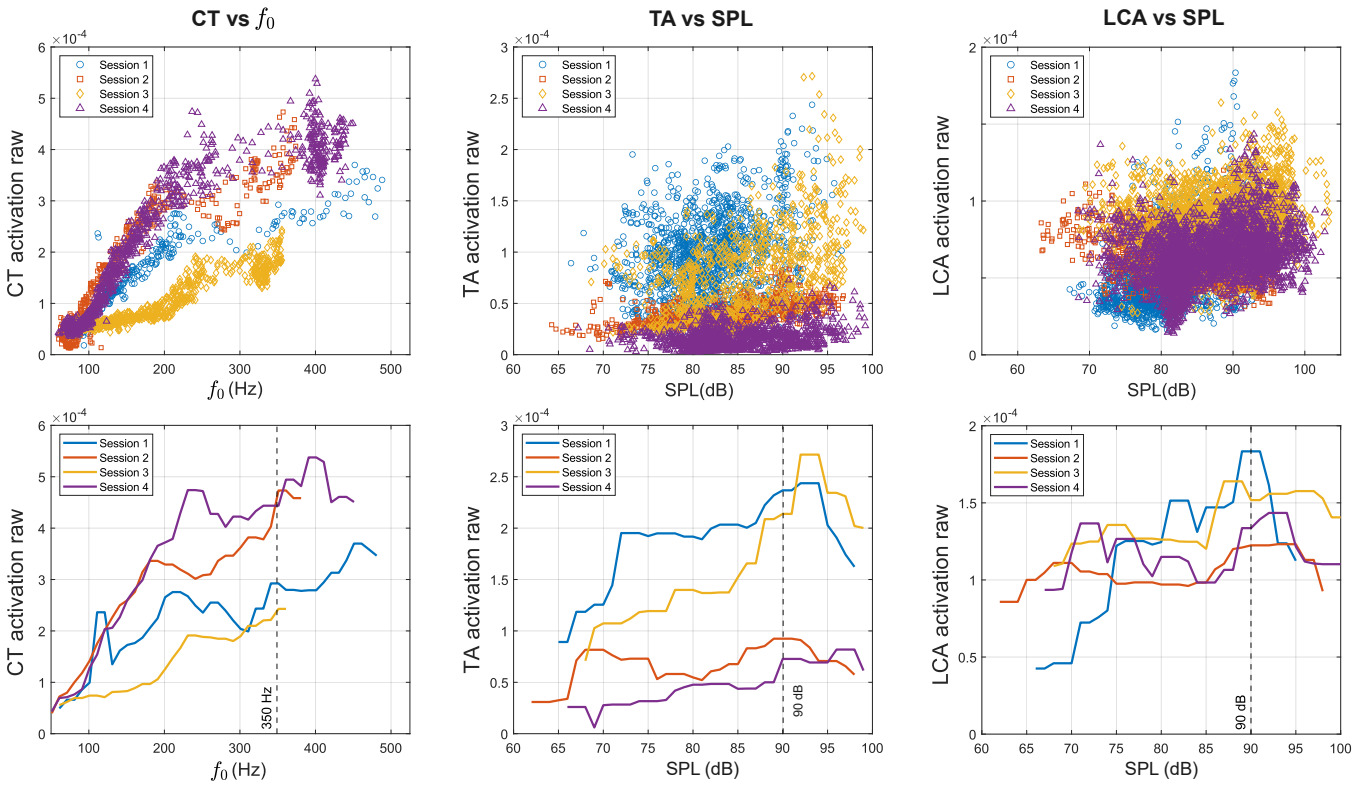

FIGURE 3. (Top row) Scatterplots showing CT activation as a function of f_o, and TA and LCA activation as a function of SPL, obtained from pitch and loudness variation tasks across the four recording sessions. (Bottom row) Maximum activation values per 1 Hz (for f_o) and 1 dB (for SPL) bin. Horizontal lines indicate the interpolated normalization values used for each session: 350 Hz for CT, and 90 dB SPL for TA and LCA.

consistently elicited high activation levels across sessions. For TA and LCA, however, the highest amplitudes were observed during non-phonatory gestures such as coughing and swallowing.

In contrast, the proposed normalization approach relied on phonatory tasks: pitch glide was used as the reference for CT, while descending loudness productions of /pae/ at low and high pitch (Phonatory Set 3) were used for TA and LCA, respectively. These phonatory conditions are illustrated in Figure 3. The top row displays scatterplots showing the relationship between EMG activation and acoustic features: CT activation versus f_o in the first column, and TA and LCA activation versus SPL in the second and third columns, respectively. The bottom row shows the discrete profiles of peak EMG activation values, constructed by grouping EMG-acoustic segments into 1 Hz bins for CT (first column) and 1 dB bins for TA and LCA (second and third columns), as described in the Methods section. For the CT muscle, a consistent increase in EMG amplitude was observed across sessions as f_o increased, displaying a linear trend up to approximately 200 Hz. Beyond this range, a transient decline in activation was noted, possibly reflecting a register transition, followed by renewed increases in amplitude, indicative of a non-linear but progressively augmenting recruitment pattern at higher f_o. In the case of the TA muscle, a moderate and consistent increase in activation with SPL was seen across all sessions, indicating a relatively stable relationship between loudness and TA engagement. For the LCA muscle, no clear or consistent trend was found across sessions. Instead, scattered peaks in activation emerged at both low and high SPL values, with variability in their positions and magnitudes across session.

These representations allow identification of the interpolated EMG amplitude corresponding to the subject-specific acoustic reference point used for normalization across the four sessions. In this case study, as highlighted by the horizontal dashed lines (Figure 3, Bottom row), the acoustic targets were set at 350 Hz for the CT muscle and 90 dB SPL for the TA and LCA muscles.These acoustic targets were selected because they represented submaximal values that were consistently achieved across all sessions, and due to their frequent use as reference maxima in computational model predictions. Linear interpolation was used as a practical approximation, under the assumption that EMG amplitude varies smoothly across small acoustic intervals. While nonlinear relationships may exist, linear interpolation was favored for its simplicity and repeatability.

Although acoustic targets (f_o = 350 Hz / SPL = 90 dB) may vary across individuals, the task-specific associations are expected to remain consistent due to shared

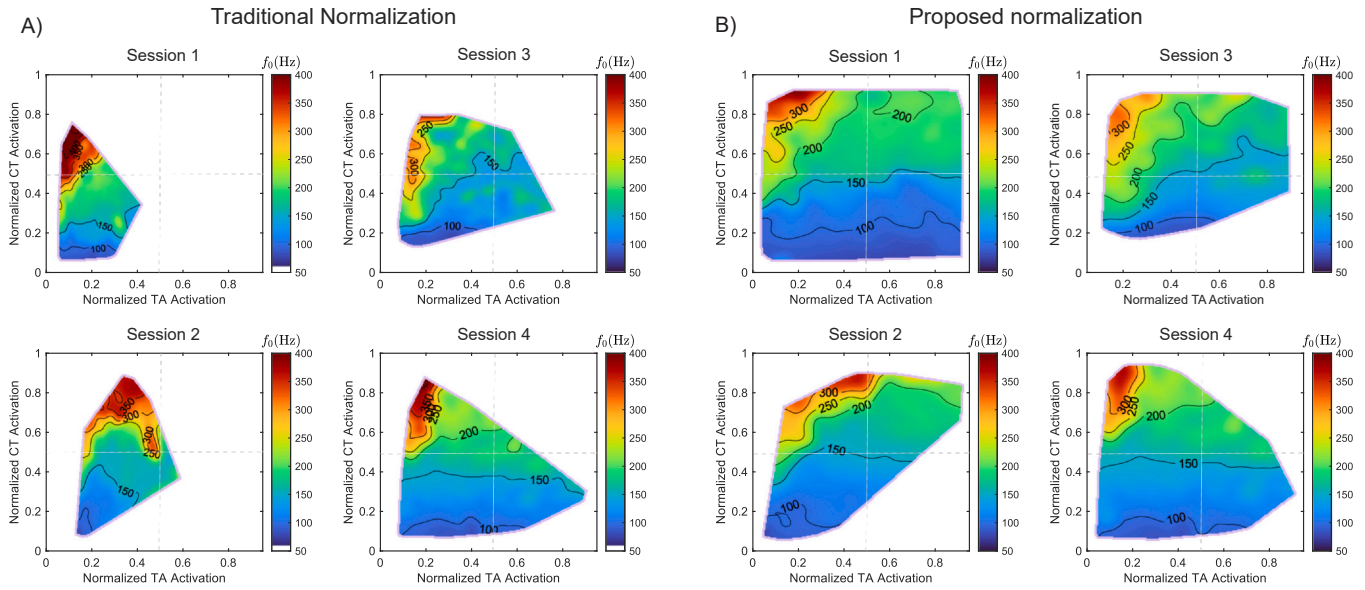

FIGURE 4. MAPs with f_o showing the relationship between normalized CT and TA muscle activation for each of the four sessions. Data points were collected from all tasks involving the vowel /a/, including sustained vowels and pitch glides, as well as the /pae/ task. The x-axis represents TA activation, while the y-axis shows CT activation, with colors indicating f_o in Hz (iso-contours indicated for f_o).

biomechanical demands, allowing submaximal acoustic targets to be adjusted to each population type.

Normalization effects on CT and TA with acoustic mapping

Figure 4 presents MAPs of f_o as a function of normalized CT and TA activation across the four recording sessions. The data were obtained from tasks involving the vowel /a/, both in sustained vowels and in pitch glide, in Phonatory Sets 1 and 2, as well as from /pae/ productions with descending loudness in Phonatory Set 3. The left MAPs were constructed using the traditional normalization, and the right ones using the proposed method.

Figure 4b shows that high f_o values (250–350 Hz) were predominantly located in the upper-left quadrant, where CT activation exceeded 0.6 and TA activation remained low to moderate ($<$ 0.5). These effects are consistent with in vivo observations in canine larynx.[8,4] In contrast, low f_o values (50–150 Hz) were distributed in the lower-left and lower-right quadrants. The upper-right quadrant, where both CT and TA were highly activated, was associated with moderate f_o values (150–250 Hz). These effects are consistent with other computer model predictions.[44,45,15] The upper-right quadrant was reached under conditions requiring increased loudness, primarily during /pae/ descending tasks, where both CT and TA showed high levels of activation. In the lower region of the MAPs, increases in TA activation under low CT conditions did not produce meaningful changes in f_o. White regions can also be observed in the contour plots, particularly more pronounced in Session 2. These areas do not reflect missing data but represent muscle coordination states that were not physiologically achieved, possibly due to differences in the fundamental frequency or loudness levels attained in each session.

Although some inter-session variation was observed, such as slightly elevated TA activation at high f_o in Session 2, the overall spatial distribution of MAPs remained stable across sessions using the proposed normalization. In contrast, MAPs generated with the traditional normalization method (Figure 4a) exhibited greater variability, with inconsistent quadrant-level patterns and reduced agreement between sessions.

These observations were supported by quantitative results presented in Table 3, with a mean r of 0.87 compared to 0.73 for the traditional method. Mean value for MAE was reduced by approximately 73% (from 70.60 Hz to 19.23 Hz), and RMSE decreased by about 72% (from 98.88 Hz to 26.98 Hz). CV dropped from 44.62% to 15.48%, and ICC(2,1) increased from 0.52 to 0.83.

Figure 5 presents MAPs of SPL as a function of normalized CT and TA activation across the four sessions, using the same data as in Figure 4. The left plots use traditional normalization, while the right plots apply the proposed method. While the proposed normalization improved intrasubject variability, the resulting SPL patterns were less sharply defined than in the CT-TA-f_o maps. SPL values above 90 dB tended to appear in regions where both CT and TA activation reached moderate to high levels, whereas values below 85 dB consistently occurred in the bottom-left quadrant, where both activations were low, consistent with prior simulation results reported.[15] In contrast, traditional normalization exhibited greater variability, with less stable contour distributions, particularly in regions of elevated TA activation.

TABLE 3.
Comparison between the traditional and the new proposed normalization in terms of *r*-value, MAE, RMSE, ICC and CV between f_o sessions.

Sessions		Traditional Normalization			New Normalization		
		(*r*)	MAE (Hz)	RMSE (Hz)	(*r*)	MAE (Hz)	RMSE (Hz)
S1	S2	0.87	59.21	75.13	0.88	17.07	25.06
S1	S3	0.77	94.04	131.84	0.85	21.86	27.19
S1	S4	0.89	61.81	88.21	0.91	17.20	22.33
S2	S3	0.49	111.24	156.77	0.83	23.63	33.13
S2	S4	0.82	44.31	67.11	0.88	20.44	26.58
S3	S4	0.53	53.02	74.22	0.84	19.18	25.58
Mean value		**0.73**	**70.60**	**98.88**	**0.87**	**19.23**	**26.98**
ICC(2,1)		**0.52**	–	–	**0.83**	–	–
CV mean (%)		**44.62**	–	–	**15.48**	–	–

As shown in Table 4 the mean *r* increased from 0.52 to 0.73. Mean MAE was reduced by 55% (from 8.20 dB to 3.66 dB), and RMSE decreased by over 58% (from 10.68 dB to 4.47 dB). The coefficient of variation dropped from 41.45% to 19.62%, representing a 52.7% reduction, and ICC(2,1) improved from 0.51 to 0.76.

Normalization effects on LCA and CT with acoustic mapping

Figure 6 presents MAPs of f_o as a function of normalized LCA and CT activation across the four recording sessions, using the same phonatory tasks as in the previous MAPs. As in earlier configurations, traditional normalization exhibited greater variability, while the proposed normalization revealed a notable expansion in the activation range of LCA, though with slightly lower consistency metrics compared to the CT-TA configurations. A consistent gradient was observed, with f_o values increasing primarily along the CT axis, while LCA activation remained relatively stable. This trend agrees with what was reported in finite element models.[17] High-frequency regions (f_o > 250 Hz) were typically associated with LCA activation above 0.4, consistent with its proposed stabilizing role during high-pitch phonation, which has been described in previous studies.[23] Notably, in Session 1, reliable MAP construction was not possible due to a failure in LCA signal acquisition during specific tasks, likely caused by poor electrode contact or insufficient signal amplitude. This prevented generation of a complete LCA-CT-f_o map for that session.

These spatial patterns were supported by the quantitative results in Table 5. The mean Pearson correlation coefficient increased from 0.88 to 0.94, reflecting a 6.8% improvement. The mean MAE decreased by 42.3%, from 35.85 Hz to 20.67 Hz, and the mean RMSE was reduced by 44.7%, from 48.63 Hz to 26.88 Hz. Additionally, ICC(2,1)

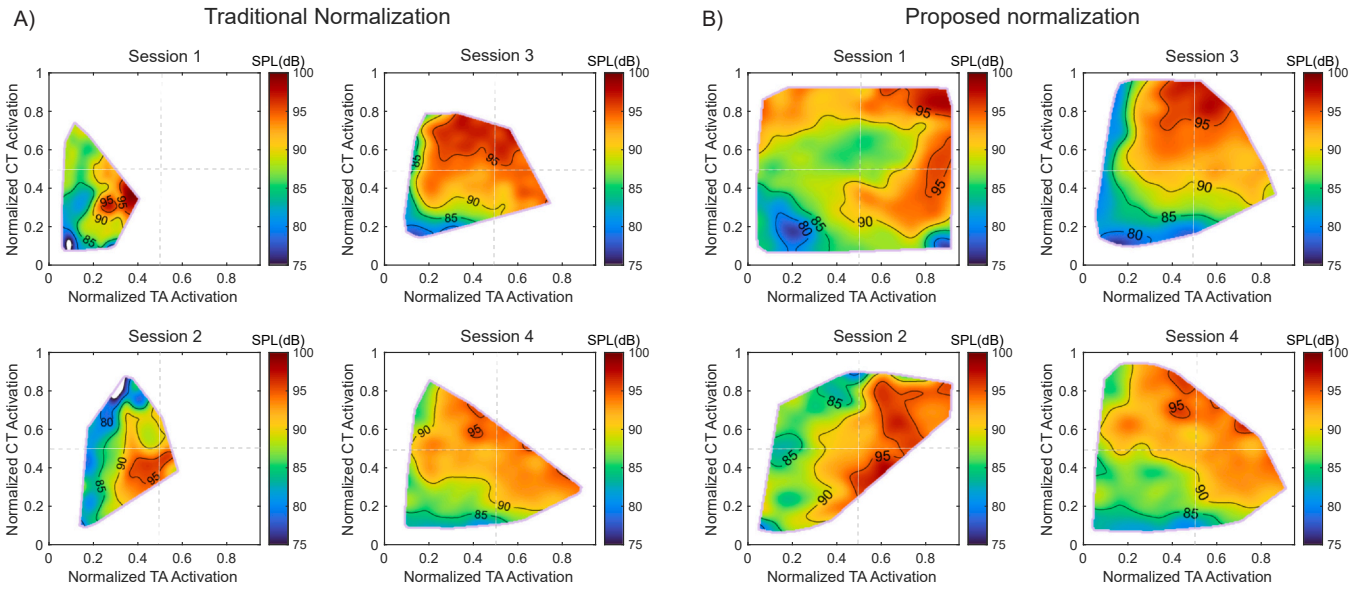

FIGURE 5. MAPs with SPL showing the relationship between normalized CT and TA muscle activation for each of the four sessions. Data points were collected from all tasks involving the vowel /a/, including sustained vowels and pitch glides, as well as the /pae/ task. The x-axis represents TA activation, while the y-axis shows CT activation, with colors indicating SPL in dB (iso-contours indicated for SPL).

TABLE 4.
Comparison between the traditional and the proposed normalization in terms of *r*-value, MAE, RMSE, ICC, and CV for SPL across sessions.

Sessions		Traditional Normalization			Proposed Normalization		
		(*r*)	MAE (dB)	RMSE (dB)	(*r*)	MAE (dB)	RMSE (dB)
S1	S2	0.77	5.79	7.33	0.85	3.96	4.69
S1	S3	0.48	8.54	10.42	0.75	4.03	4.84
S1	S4	0.58	7.81	9.62	0.72	3.14	3.70
S2	S3	0.10	13.46	17.11	0.54	4.52	5.65
S2	S4	0.30	9.97	12.82	0.60	3.78	4.71
S3	S4	0.89	3.63	4.77	0.93	2.51	3.22
Mean		**0.52**	**8.20**	**10.68**	**0.73**	**3.66**	**4.47**
ICC(2,1)		**0.51**	–	–	**0.76**	–	–
CV (%)		**41.45**	–	–	**19.62**	–	–

increased from 0.744 to 0.869, and the coefficient of variation (CV) dropped from 25.20% to 15.60%, reflecting a 38.1% reduction.

DISCUSSION

Compared to traditional peak-based normalization, the proposed method produced more consistent spatial patterns across sessions in all three activation-acoustic MAP configurations. Instead of relying on arbitrary peak values, which can vary even within the same participant across sessions, as observed in this study, the method bases normalization to submaximal muscle activation levels recorded during tasks and acoustic targets with strong physiological coupling. By standardizing activation across tasks and sessions, this approach improves the consistency of EMG data and enhances its utility in downstream applications, including optimization of numerical biomechanical

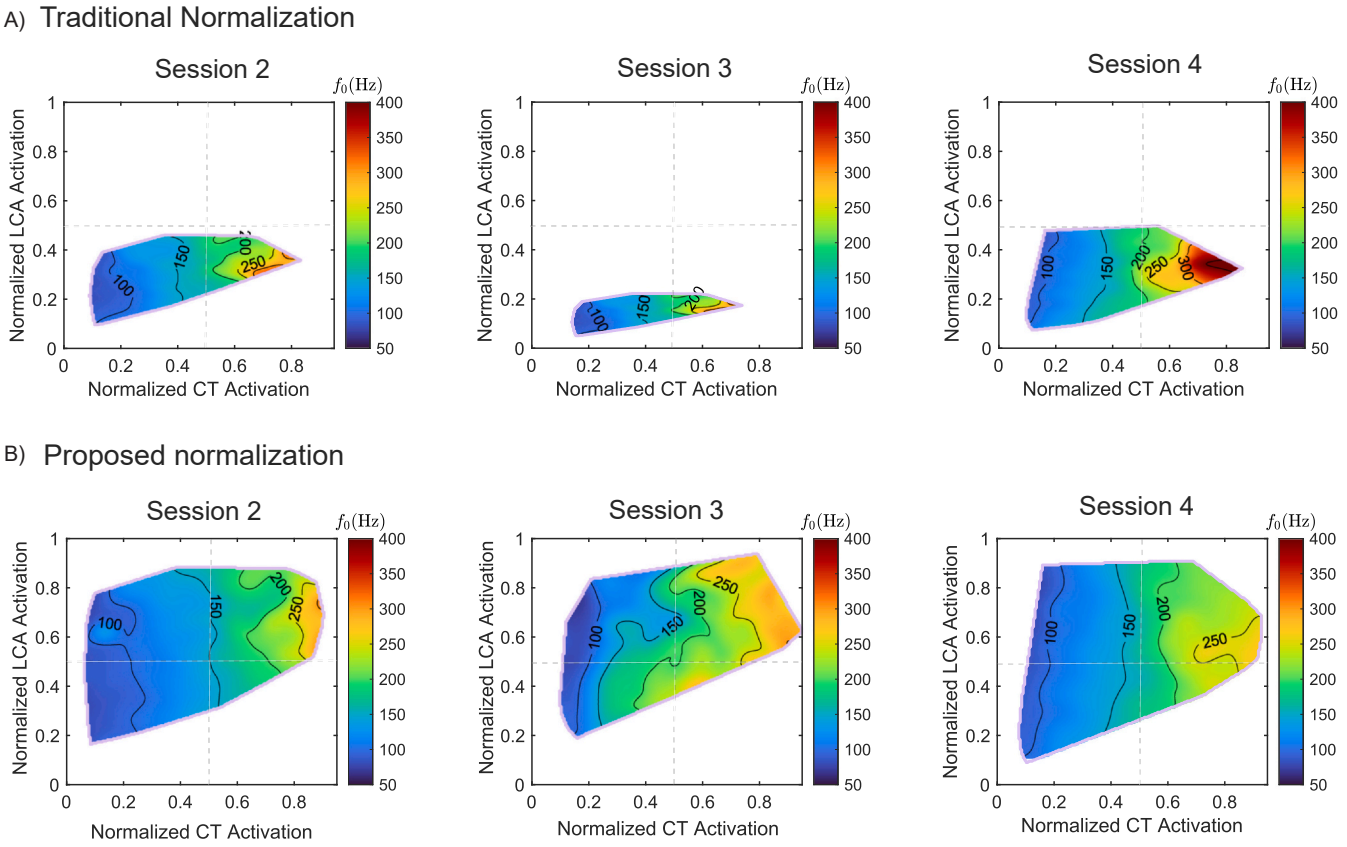

FIGURE 6. MAPs with f_o showing the relationship between normalized LCA and CT muscle activation for each of the four sessions. Data points were collected from all tasks involving the vowel /a/, including sustained vowels and pitch glides, as well as the /pae/ task. The x-axis represents CT activation, while the y-axis shows LCA activation, with colors indicating f_o in Hz (iso-contours indicated for f_o).

TABLE 5.
Comparison between the traditional and the new proposed normalization in terms of *r*-value, MAE, RMSE, ICC, and CV between f_o sessions for the LCA-CT condition. Only sessions 2 to 4 were included.

Sessions		Traditional Normalization			New Normalization		
		(*r*)	MAE (Hz)	RMSE (Hz)	(*r*)	MAE (Hz)	RMSE (Hz)
S2	S3	0.8082	41.84	54.63	0.9484	26.03	32.81
S2	S4	0.9295	39.08	54.38	0.9570	18.75	23.24
S3	S4	0.8933	26.65	36.89	0.9291	17.23	24.58
Mean value		**0.88**	**35.85**	**48.63**	**0.94**	**20.67**	**26.88**
ICC(2,1)		**0.744**	–	–	**0.869**	–	–
CV (%)		**25.20**	–	–	**15.60**	–	–

modeling[46,47] and machine learning-based regression pipelines for estimating voice-related features.[18,48,49] In this sense, the normalized data may serve as a valuable bridge between experimental recordings and theoretical modeling frameworks.

Cross-correlation and *r*-value analyses were useful tools for refining channel selection and verifying muscle identity. In particular, the descending pitch glide task consistently revealed negative correlations between CT and TA channels, which aided in reclassifying mislabeled electrodes. For example, in Session 4 (Figure 1), one channel initially identified as CT showed stronger correlation patterns with TA, suggesting a misplacement. Additionally, high cross-correlation values supported the identification of electrode pairs inserted in close proximity within the same muscle, providing useful feedback in a procedure that is often performed with limited visual guidance.

The association between CT activation and increases in f_o was consistently observed across all sessions (Figure 4), reinforcing its biomechanical role in VF elongation and tension control. TA activation was essential under high-pressure conditions, as reflected in the upper-right quadrant of the CT-TA MAPs, which was only reached during the /pae/ descending loudness task. In this region, moderate f_o values (150–200 Hz) were observed, suggesting that TA did not drive pitch increases but instead supported phonatory stability through its role in achieving complete glottal closure and enabling higher P_s, as reported in previous studies.[9] When compared to simulations results,[16,15,11] the isocontour spacing observed here showed increased separation between 150 and 200 Hz, and reduced spacing between 250 and 300 Hz, indicating a less uniform frequency distribution than that generated by the models. These differences may be attributed to subject-specific anatomical characteristics, as well as to the choice of acoustic reference values used for normalization in this study.

Although the LCA did not exhibit strong directional influence over f_o trajectories, its persistent activation in high-pitch contexts likely reflects its consistent adductory function during phonation, which appears to be less affected by pitch or loudness modulation demands and instead supports a complementary biomechanical role in maintaining glottal configuration. This interpretation is consistent with previous findings indicating that LCA contraction increases glottal closure without significantly altering vocal fold longitudinal stiffness.[23,17] Moreover, the reduced intrasubject variability observed with the proposed normalization supports the notion that LCA activity is less sensitive to task-specific demands. This is further reinforced by the limited variation in its maximal activation across both phonatory tasks (Figure 3), especially when compared to the CT and TA muscles. Such a reduced dynamic range may underlie the spatial uniformity observed in LCA MAPs (Figure 6). The spatial organization observed in these MAPs aligns with physiological expectations regarding the functional interplay between the elongator (CT) and the adductor (LCA) muscles.[2] These findings also suggest that SPL may be biomechanically misaligned with LCA function, indicating that it may not be an adequate normalization target for this muscle. Alternative strategies that better reflect its adductory role or coordination with TA may be needed.

As shown in the MAPs (Figure 5), after normalization, the SPL surface within the CT-TA activation space displays an expanded and continuous representation, with values ranging from approximately 75 to 100 dB SPL, which is well within a physiologically meaningful range given the microphone distance. The contours show gradual and consistent increases in SPL with increasing TA and CT activation, consistent with expected biomechanical relationships.[28,27] Although the spatial distribution is less efficient than with f_o, the normalized map reflects one of the expected outcomes of the framework: improved continuity and coverage of the activation space across sessions. The increased area of valid data points and the smoother contour progression suggest better alignment between muscle activation and acoustic output.

These findings highlight the potential clinical relevance of acoustic-based normalization in laryngeal EMG. Although the protocol is technically demanding and not yet intended for routine clinical use, it establishes a physiologically grounded framework that addresses session-to-session variability, one of the central limitations of laryngeal EMG. Accordingly, acoustic-based normalization may serve as a useful approach for monitoring neuromuscular

changes over time in clinical populations, for instance, in pre- and post-therapy or surgical assessments. In future work, the experimental protocol and proposed method may also support enhancements to computational models, making them more physiologically representative and enabling non-invasive, routine clinical estimation of laryngeal EMG.

Limitations

The analysis was conducted on a single participant, an older adult male, which limits the generalization of the findings. Anatomical and physiological variability across different populations, including individuals with vocal pathologies or altered laryngeal function, cannot be addressed at this point. Caution should therefore be exercised when extrapolating these results beyond the specific conditions of this case.

In both f_o and SPL distributions, some sessions exhibited white regions in the CT-TA activation space, particularly in the bottom-right quadrant where CT activation was low and TA activation exceeded 0.6. This suggests that high TA activation in isolation may be insufficient to produce phonation.[1] These gaps indicate that the participant did not consistently reach the same f_o and SPL with combinations of CT, TA, LCA, and P_s on different recording days. This highlights the degree of intra-subject variability, even when performing standardized phonatory tasks in separate sessions. Such variability may limit the representation of the full muscle activation space and should be considered when designing protocols or interpreting EMG data. It should also be noted that the pitch glide tasks were performed at a comfortable loudness level, limiting the range of Ps modulation and the full extent of CT-TA-SPL interactions.

Regarding the LCA muscle activation, the normalization approach based on SPL was less effective. As shown in Table 5, only modest improvements were observed in ICC and variability metrics, compared to the more pronounced gains seen for CT and TA. These findings suggest that SPL-based normalization may not be as suitable for LCA muscle.

Another limitation lies in the use of a fixed acoustic target as a basis for normalization. While these values were consistently achieved in this study, they may not be attainable in other populations, particularly in individuals with reduced vocal capacity. As such, data from additional participants will be necessary to validate or refine these reference values and assess the broader applicability of the method.

Finally, future studies should consider incorporating pitch glide tasks performed at multiple loudness levels to better capture frequency variation under different P_s. Such tasks could enrich the representation of muscle activation patterns and improve the robustness of the normalization framework.

CONCLUSIONS

This study presents a step toward the standardization of intramuscular EMG normalization in the larynx by proposing a physiologically grounded method based on interpolated muscle activation at fixed acoustic targets. The approach demonstrated improved consistency across sessions for CT, TA and LCA muscles, facilitating the MAPs patterns relative to pitch and loudness.

Although the method was evaluated in repeated sessions from a single participant, the observed patterns align with known functional roles of ILM and provide insight into muscle-specific contributions under varying acoustic conditions. Future studies involving multiple participants and broader task protocols will be essential to refine this framework and evaluate its applicability across populations. This work contributes to establishing methodological guidelines for EMG normalization and supports further investigation into neuromuscular control strategies in voice production.

Ethics approval

Informed consent was obtained from the participant, and the experimental protocols were approved by the institutional review board of the Massachusetts General Hospital, Boston (Protocol 2008P000652).

Data availability

De-identified overall average values for variables in this study are included as Figures. Because these data are from a human subject, more detailed data may be available upon request, if appropriate, and require a data use agreement. Anyone wishing to request access to the data must first contact Ms. Sarah DeRosa, Program Coordinator for Research and Clinical Speech-Language Pathology, Center for Laryngeal Surgery and Voice Rehabilitation, Massachusetts General Hospital: sederosa@partners.org.

Declaration of Competing Interests

The authors declare the following financial interests/personal relationships which may be considered as potential competing interests: Matías Zañartu reports financial support was provided by National Institutes of Health (NIH), National Institute on Deafness and Other Communication Disorders grant P50DC01544. Matías Zañartu reports financial support was provided by National Agency for Research and Innovation (ANID) grants FONDECYT projects 1230828, and BASAL. Emiro Ibarra reports financial support from ANID through FONDECYT Postdoctoral Project No. 3250844. Josué Martinez reports financial support was provided by Federico Santa Maria Technical University, DPP PIIC 036/2023. Robert Hillman reports a relationship with InnoVoyce LLC that includes: equity or stocks. Daryush Mehta reports a relationship with InnoVoyce LLC that includes: equity or stocks. Matías Zañartu reports a

relationship with Lanek SPA that includes: equity or stocks. If there are other authors, they declare that they have no known competing financial interests or personal relationships that could have appeared to influence the work reported in this paper.

Acknowledgments

This research was supported by the National Institutes of Health (NIH) National Institute on Deafness and Other Communication Disorders grant P50DC015446, ANID grants FONDECYT projects 1230828, 3250844, and BASAL AFB240002, UTFSM grant DPP PIIC 036/2023. The content is solely the responsibility of the authors and does not necessarily represent the official views of the NIH.
a) Correspondence concerning this article should be addressed to Matías Zañartu, Department of Electronic Engineering and Advanced Center for Electrical and Electronic Engineering, Universidad Técnica Federico Santa María, Valparaíso, Chile, Avda. España 1680. E-mail: matias.zanartu@usm.cl.

Disclosure

Drs. Robert Hillman and Daryush Mehta have a financial interest in InnoVoyce LLC, a company focused on developing and commercializing technologies for the prevention, diagnosis, and treatment of voice-related disorders. Dr. Hillman's and Dr. Mehta's interests were reviewed and are managed by Massachusetts General Hospital and Mass General Brigham in accordance with their conflict-of-interest policies. Dr. Matías Zañartu has financial interest in Lanek SPA, a company focused on developing and commercializing biomedical devices and technologies. Dr. Zañartu's interests were reviewed and are managed by Universidad Técnica Federico Santa María in accordance with its conflict-of-interest policies.

REFERENCES

1. Titze IR, Luschei ES, Hirano M. Role of the thyroarytenoid muscle in regulation of fundamental frequency. *Journal of Voice.* 1989;3(3):213–224. https://doi.org/10.1016/S0892-1997(89)80003-7.
2. Titze IR, Sundberg J. Vocal intensity in speakers and singers. *the Journal of the Acoustical Society of America.* 1992;91(5):2936–2946. https://doi.org/10.1121/1.402929.
3. Titze IR, Hunter EJ. A two-dimensional biomechanical model of vocal fold posturing. *The Journal of the Acoustical Society of America.* 2007;121(4):2254–2260. https://doi.org/10.1121/1.2697573.
4. Chhetri DK, Neubauer J, Berry DA. Neuromuscular control of fundamental frequency and glottal posture at phonation onset. *The Journal of the Acoustical Society of America.* 2012;131(2):1401–1412. https://doi.org/10.1121/1.3672686.
5. Choi HS, Ye M, Berke GS. Function of the interarytenoid(IA) muscle in phonation: in vivo laryngeal model. *Yonsei Medical Journal.* 1995;36(1):58–67. https://doi.org/10.3349/ymj.1995.36.1.58.
6. Choi H-S, Berke GS, Ye M, Kreiman J. Function of the posterior cricoarytenoid muscle in phonation: In vivo laryngeal model. *Otolaryngology-Head and Neck Surgery.* 1993;109(6):1043–1051. https://doi.org/10.1177/019459989310900612.
7. Cox K, Alipour F, Titze I. Geometric Structure of the Human and Canine Cricothyroid and Thyroarytenoid Muscles for Biomechanical Applications. *The Annals of otology, rhinology, and laryngology.* 1999;108(12):1151–1158. https://doi.org/10.1177/000348949910801210.
8. Chhetri DK, Neubauer J, Sofer E, Berry DA. Influence and interactions of laryngeal adductors and cricothyroid muscles on fundamental frequency and glottal posture control. *The Journal of the Acoustical Society of America.* 2014;135(4):2052–2064. https://doi.org/10.1121/1.4865918.
9. Chhetri DK, Neubauer J. Differential Roles for the Thyroarytenoid and Lateral Cricoarytenoid Muscles in Phonation. *The Laryngoscope.* 2015;125(12):2772. https://doi.org/10.1002/lary.25480.
10. Chhetri DK, Park SJ. Interactions of subglottal pressure and neuromuscular activation on fundamental frequency and intensity. *The Laryngoscope.* 2016;126(5):1123–1130. https://doi.org/10.1002/lary.25550.
11. Titze IR, Story BH. Rules for controlling low-dimensional vocal fold models with muscle activation. *The Journal of the Acoustical Society of America.* 2002;112(3):1064–1076. https://doi.org/10.1121/1.1496080.
12. Farley GR. A biomechanical laryngeal model of voice F_0 and glottal width control. *The Journal of the Acoustical Society of America.* 1996;100(6):3794–3812. https://doi.org/10.1121/1.417218.
13. Lowell S, Story B. Simulated effects of cricothyroid and thyroarytenoid muscle activation on adult-male vocal fold vibration. *The Journal of the Acoustical Society of America.* 2006;120(1):386–397. https://doi.org/10.1121/1.2204442.
14. Hunter EJ, Titze IR, Alipour F. A three-dimensional model of vocal fold abduction/adduction. *The Journal of the Acoustical Society of America.* 2004;115(4):1747–1759. https://doi.org/10.1121/1.1652033.
15. Palaparthi A, Smith S, Titze IR. Mapping thyroarytenoid and cricothyroid activations to postural and acoustic features in a fiber-gel model of the vocal folds. *Applied Sciences.* 2019;9(21):4671. https://doi.org/10.3390/app9214671.
16. Alzamendi GA, Peterson SD, Erath BD, Hillman RE, Zañartu M. Triangular body-cover model of the vocal folds with coordinated activation of the five intrinsic laryngeal muscles. *The Journal of the Acoustical Society of America.* 2022;151(1):17–30. https://doi.org/10.1121/10.0009169.
17. Yin J, Zhang Z. Interaction Between the Thyroarytenoid and Lateral Cricoarytenoid Muscles in the Control of Vocal Fold Adduction and Eigenfrequencies. *Journal of Biomechanical Engineering.* 2014;136(11):111006. https://doi.org/10.1115/1.4028428.
18. Ibarra EJ, Parra JA, Alzamendi GA, Cortés JP, Espinoza VM, Mehta DD, Hillman RE, Zañartu M. Estimation of Subglottal Pressure, Vocal Fold Collision Pressure, and Intrinsic Laryngeal Muscle Activation From Neck-Surface Vibration Using a Neural Network Framework and a Voice Production Model. *Frontiers in Physiology.* 2021;12:732244. https://doi.org/10.3389/fphys.2021.732244.
19. Manriquez R, Peterson SD, Prado P, Orio P, Galindo GE, Zañartu M. Neurophysiological Muscle Activation Scheme for Controlling Vocal Fold Models. *IEEE transactions on neural systems and rehabilitation engineering: a publication of the IEEE Engineering in Medicine and Biology Society.* 2019;27(5):1043–1052. https://doi.org/10.1109/TNSRE.2019.2906030.
20. Erath BD, Zañartu M, Peterson SD, Plesniak MW. Nonlinear vocal fold dynamics resulting from asymmetric fluid loading on a two-mass model of speech. *Chaos.* 2011;21(3):033113. https://doi.org/10.1063/1.3615726.
21. Gay T, Strome M, Hirose H, Sawashima M. Electromyography of the Intrinsic Laryngeal Muscles during Phonation. (publisher: SAGE Publications Inc). *Annals of Otology, Rhinology & Laryngology.* 1972;81(3):401–409. https://doi.org/10.1177/000348947208100311.
22. Hillel AD. The Study of Laryngeal Muscle Activity in Normal Human Subjects and in Patients With Laryngeal Dystonia Using Multiple Fine-Wire Electromyography. *The Laryngoscope.* 2001;111(S97):1–47. https://doi.org/10.1097/00005537-200104001-00001.

23. Hirano M, Ohala J, Vennard W. The Function of Laryngeal Muscles in Regulating Fundamental Frequency and Intensity of Phonation. (publisher: American Speech-Language-Hearing Association). *Journal of Speech and Hearing Research.* 1969;12(3):616–628. https://doi.org/10.1044/jshr.1203.616.
24. Poletto CJ, Verdun LP, Strominger R, Ludlow CL. Correspondence between laryngeal vocal fold movement and muscle activity during speech and nonspeech gestures. (publisher: American Physiological Society). *Journal of Applied Physiology.* 2004;97(3):858–866. https://doi.org/10.1152/japplphysiol.00087.2004.
25. Kochis-Jennings KA, Finnegan EM, Hoffman HT, Jaiswal S. Laryngeal muscle activity and vocal fold adduction during chest, chestmix, headmix, and head registers in females. *Journal of Voice.* 2012;26(2):182–193. https://doi.org/10.1016/j.jvoice.2010.11.002.
26. Roubeau B, Chevrie-Muller C, Saint Guily JL. Electromyographic activity of strap and cricothyroid muscles in pitch change. *Acta oto-laryngologica.* 1997;117(3):459–464. https://doi.org/10.3109/00016489709113421.
27. Finnegan EM, Luschei ES, Hoffman HT. Modulations in respiratory and laryngeal activity associated with changes in vocal intensity during speech. *Journal of Speech, Language, and Hearing Research.* 2000;43(4):934–950. https://doi.org/10.1044/jslhr.4304.934.
28. Baker KK, Ramig LO, Sapir S, Luschei ES, Smith ME. Control of vocal loudness in young and old adults. *Journal of Speech, Language, and Hearing Research.* 2001;44(2) https://doi.org/10.1044/1092-4388(2001/024).
29. Merletti R, DiTorino P. Standards for reporting emg data. *Journal of Electromyography and Kinesiology.* 1999;9(1):3–4.
30. Kochis-Jennings KA, Finnegan EM, Hoffman HT, Jaiswal S, Hull D. Cricothyroid muscle and thyroarytenoid muscle dominance in vocal register control: preliminary results. *Journal of Voice.* 2014;28(5):652–e21. https://doi.org/10.1016/j.jvoice.2014.01.017.
31. Tabard-Fougère A, Rose-Dulcina K, Pittet V, Dayer R, Vuillerme N, Armand S. Emg normalization method based on grade 3 of manual muscle testing: Within-and between-day reliability of normalization tasks and application to gait analysis. *Gait & posture.* 2018;60:6–12. https://doi.org/10.1016/j.gaitpost.2017.10.026.
32. Burden A. How should we normalize electromyograms obtained from healthy participants? What we have learned from over 25 years of research. *Journal of electromyography and kinesiology.* 2010;20(6):1023–1035. https://doi.org/10.1016/j.jelekin.2010.07.004.
33. Hirano M, Ohala J, Vennard W. The function of laryngeal muscles in regulating fundamental frequency and intensity of phonation. *Journal of Speech and Hearing Research.* 1969;12(3):616–628. https://doi.org/10.1044/jshr.1203.616.
34. Ludlow CL. Central nervous system control of the laryngeal muscles in humans. *Respiratory physiology & neurobiology.* 2005;147(2-3):205–222. https://doi.org/10.1016/j.resp.2005.04.015.
35. Hirano M, Ohala J. Use of Hooked-Wire Electrodes for Electromyography of the Intrinsic Laryngeal Muscles. (publisher: American Speech-Language-Hearing Association). *Journal of Speech and Hearing Research.* 1969;12(2):362–373. https://doi.org/10.1044/jshr.1202.362.
36. Volk GF, Hagen R, Pototschnig C, Friedrich G, Nawka T, Arens C, Mueller A, Foerster G, Finkensieper M, Lang-Roth R, Sittel C, Storck C, Grosheva M, Kotby MN, Klingner CM, Guntinas-Lichius O. Laryngeal electromyography: a proposal for guidelines of the European Laryngological Society. *European Archives of Oto-Rhino-Laryngology.* 2012;269(10):2227–2245. https://doi.org/10.1007/s00405-012-2036-1.
37. Rossing T. *Springer handbook of acoustics.* Springer Science & Business Media; 2007.
38. Hermes DJ. Measurement of pitch by subharmonic summation. *The journal of the acoustical society of America.* 1988;83(1):257–264. https://doi.org/10.1121/1.396427.
39. Dewald HA, Lukyanenko P, Lambrecht JM, Anderson JR, Tyler DJ, Kirsch RF, Williams MR. Stable, three degree-of-freedom myoelectric prosthetic control via chronic bipolar intramuscular electrodes: a case study. *Journal of neuroengineering and rehabilitation.* 2019;16(147):1–13. https://doi.org/10.1186/s12984-019-0607-8.
40. Lowery MM, Stoykov NS, Kuiken TA. A simulation study to examine the use of cross-correlation as an estimate of surface emg cross talk. *Journal of Applied Physiology.* 2003;94(4):1324–1334. https://doi.org/10.1152/japplphysiol.00698.2002.
41. Hirano M, Vennard W, Ohala J. Regulation of register, pitch and intensity of voice: An electromyographic investigation of intrinsic laryngeal muscles. *Folia phoniatrica et logopaedica.* 1970;22(1):1–20. https://doi.org/10.1159/000263363.
42. Chuang TD, Acker SM. Comparing functional dynamic normalization methods to maximal voluntary isometric contractions for lower limb emg from walking, cycling and running. *Journal of electromyography and kinesiology.* 2019;44:86–93. https://doi.org/10.1016/j.jelekin.2018.11.014.
43. Knutson LM, Soderberg GL, Ballantyne BT, Clarke WR. A study of various normalization procedures for within day electromyographic data. *Journal of electromyography and kinesiology.* 1994;4(1):47–59. https://doi.org/10.1016/1050-6411(94)90026-4.
44. Jiang W, Geng B, Zheng X, Xue Q. A computational study of the influence of thyroarytenoid and cricothyroid muscle interaction on vocal fold dynamics in an mri-based human laryngeal model. *Biomechanics and Modeling in Mechanobiology.* 2024;23(5):1801–1813. https://doi.org/10.1007/s10237-024-01869-9.
45. Movahhedi M, Geng B, Xue Q, Zheng X. Effects of cricothyroid and thyroarytenoid interaction on voice control: Muscle activity, vocal fold biomechanics, flow, and acoustics. *The Journal of the Acoustical Society of America.* 2021;150(1):29–42. https://doi.org/10.1121/10.0005275.
46. Alzamendi GA, Manríquez R, Hadwin PJ, Deng JJ, Peterson SD, Erath BD, Mehta DD, Hillman RE, Zañartu M. Bayesian estimation of vocal function measures using laryngeal high-speed videoendoscopy and glottal airflow estimates: An in vivo case study. *The Journal of the Acoustical Society of America.* 2020;147(5):EL434–EL439. https://doi.org/10.1121/10.0001276.
47. Ibarra EJ, Alzamendi GA, Zañartu M. Constrained extended Kalman filter for improving Bayesian inference of vocal function from laryngeal high-speed videoendoscopy. In: 18th International Symposium on Medical Information Processing and Analysis. 2023; 12567: 125671E. https://doi.org/10.1117/12.2669812.
48. Ibarra EJ, Arias-Londoño JD, Godino-Llorente JI, Mehta DD, Zañartu M. Subject-specific modeling by domain adaptation for the estimation of subglottal pressure from neck-surface acceleration signals, Biomedical. *Signal Processing and Control.* 2025;106:107681. https://doi.org/10.1016/j.bspc.2025.107681.
49. Sepúlveda J, Parra JA, Ibarra EJ, Araya M, Cuadra PDL, Zañartu M. Estimation of physiological vocal features from neck surface acceleration signals using probabilistic bayesian neural networks. *IEEE Transactions on Audio, Speech and Language Processing.* 2025;33:1576–1589. https://doi.org/10.1109/TASLPRO.2025.3552938.